International Journal of Control and Automation
Vol.7, No.5 (2014), pp.77-86
http://dx.doi.org/10.14257/ijca.2014.7.5.09

# Research on Dynamic Decoupling Control Method of Three-phase Bearingless Induction Motor

Wen-shao Bu, Chun-xiao Lu, Cong-lin Zu and Xin-wen Niu

*College of Information Engineering, Henan University of Science and Technology, Luoyang, 471023, China*
*wsbu@163.com*

***Abstract***

*Three-phase bearingless induction motor is a multi-variable, nonlinear and strong coupling object, to achieve its high performance control, the dynamic mathematical models was analyzed firstly. According to the derived mathematical model, the reversibility of bearingless induction motor system was discussed, and the dynamic mathematical models of inverse system were derived. Then, based on the inverse system method, the dynamic decoupling control strategy of three-phase bearingless induction motor was researched, and the dynamic decoupling control system was build. Simulation results show that the dynamic decoupling control has been achieved between motor speed, rotor flux linkage and two radial displacement components, and the control system has higher dynamic and static performance; the presented decoupling control method is effective and feasible.*

***Keywords:*** *Three-phase Bearingless Induction Motor; Dynamic Decoupling Control Strategy; Rotor Flux Orientation; Inverse System Method; Mathematical Model*

## 1. Introduction

Motor with magnetic bearings has been developed and widely used in high-speed drive kingdoms. But, the motor with magnetic bearings has a series of disadvantages, such as: longer rotor shaft, higher magnetic suspensions cost, difficulty to over speed, etc. [1, 2]. Based on the comparability in configuration between magnetic bearing and conventional motor stator, the bearingless motor is proposed, which embeds the windings of magnetic bearing in the stator slots along with the conventional motor windings. Bearingless motor is a newly type of electric machinery, which not only has the function of conventional motor, but also has the self-suspension function. Compared with the motor with magnetic bearings, the bearingless motor has a series of advantages, such as shorter rotor shaft, higher critical speed, being applicable to super-high speed and long time running [1-6]. Bearingless control technology can be used to all kinds of AC motors [1-3].

Bearingless induction motor not only has the advantages of other bearingless motors, but also has the compact and robust structure, then owns broad application prospects [1, 4- 8]. But, there exist complex electromagnetic coupling relations within bearingless induction motor. Then, to achieve its high performance control, it is necessary to achieve the dynamic decoupling between all state variables of bearingless induction motor.

Inverse system method is direct feedback linearization method that be proposed according to complex nonlinear system in recent years. The basic idea of inverse system method can be summarized as following: based on the mathematical model of original system, the mathematical model of inverse system is build; and the original system will be compensated

ISSN: 2005-4297 IJCA

to several decoupled pseudo linear subsystems. Then, using various design methods of linear systems theory, the controller of each pseudo linear subsystem can be designed [9]. About the inverse system decoupling control of bearingless induction motor, there have been preliminary researches [9, 10]. But, the current research always define the motor equations in two-phase synchronous reference frame, the solution process of inverse system model is complicated and is not convenient for application. To simplify the mathematical model of bearingless induction motor, the paper will define the bearingless induction motor in the reference frame orientated by rotor flux-linkage, and take the stator currents as input variables. Then, adopting inverse system method, the controlled object will be decoupled to four linear integral subsystems, including motor speed, rotor flux-linkage and two radial displacement components. And by way of design methods of linear systems theory, integrated designs of four linear integral subsystems will be made, and the dynamic decoupling control with high performance of three-phase bearingless induction motor will be achieved.

## 2. Dynamic Mathematical Model of Bearingless Inducion Motor

### 2.1 Working principle of bearingless motor

There are two sets of windings in stator slots of bearingless motor, including torque windings whose number of pole pairs is $p_1$ and its electrical angle frequency is $\omega_1$, and suspension control windings whose number of pole pairs is $p_2$ and its electrical angle frequency is $\omega_2$.

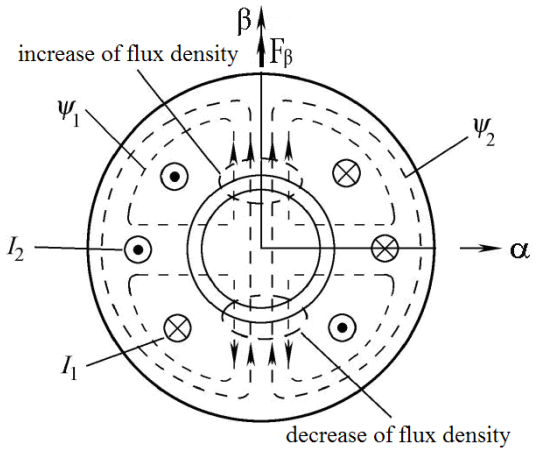


**Figure 1. Sketch map of working principle for bearingless motor**

The torque windings will produce rotate magnetic field of conventional motor that be used to realize rotary drive of rotor; the suspension control windings will produce another set of rotate magnetic field that be used to control the radial suspension of rotor. When the suspension control magnetic field is superimposed on the motor magnetic field, the magnetic field in some airgap area will be increased, and that in its spatial symmetrical airgap area will be weakened. When the numbers of pole pairs and the electrical angle frequencies of two sets of windings meet the qualification of "$p_2=p_1\pm1$, $\omega_1=\omega_2$", the radial magnetic suspension force can be produced whose amplitude and direction can be controlled stably. The controllable magnetic suspension force can be used to control the suspension of rotor. That is known as the working principle of bearingless motor.

Figure 1 shows the production principle of controllable magnetic suspension force of four-pole bearingless motor with two-pole suspension windings. On the moment that stator current

 

of two sets of windings are as shown in Figure 1, the stable controllable magnetic suspension force $F_\alpha$ will be produced.

### 2.2 Dynamical mathematical models of three-phase bearingless induction motor

For bearingless induction motor, the production principle of electromagnetic torque is the same with conventional motor. To simplify the mathematical model of bearingless induction motor, the stator current of toque system will be taken as control variable. Then, the dynamic model of four-pole torque system in *d-q* synchronous reference frame can be derived as following:

$$\dot{\psi}_{rd} = -\psi_{rd}/T_r + (\omega_1 - \omega_r)\psi_{rq} + L_{m1}i_{s1d}/T_r \tag{1}$$

$$\dot{\psi}_{rq} = -\psi_{rq}/T_r - (\omega_1 - \omega_r)\psi_{rd} + L_{m1}i_{s1q}/T_r \tag{2}$$

$$\dot{\omega}_r = p_1^2 L_{m1}(\psi_{rd}i_{s1q} - \psi_{rq}i_{s1d})/(JL_r) - p_1 T_L / J \tag{3}$$

In equations (1)~(3): $\omega_r$ is the motor speed; $\omega_1$ is the synchronous electrical angle frequency of *d-q* reference frame; $\psi_{rd}$ and $\psi_{rq}$ are two rotor flux-linkage components of torque system along *d* and *q* reference axes; $i_{s1d}$ and $i_{s1q}$ are two current components of torque windings along *d* and *q* reference axes; $L_{m1}$ is the excited inductance of torque windings; $L_r$ is the self-inductance of equivalent two-phase rotor windings; *J* is the rotor's rotation inertia; $T_L$ is the load torque.

If the *d-q* reference frame is oriented by the rotor flux-linkage vector of torque system, there will exist relationships of "$\psi_r = \psi_{rd}$, $\psi_{rq} = \dot{\psi}_{rq} = 0$". Put the relation equations into equation (1), then following equations can be derived:

$$\dot{\psi}_r = -\psi_r/T_r + L_{m1}i_{s1d}/T_r \tag{4}$$

$$\omega_s = \omega_1 - \omega_r = L_{m1}i_{s1q}/(T_r\psi_r) \tag{5}$$

$$\dot{\omega}_r = p_1^2 L_{m1}\psi_r i_{s1q}/(JL_r) - p_1 T_L / J \tag{6}$$

For two-pole magnetic suspension system, the mathematical model of controllable radial magnetic suspension force can be expressed as following [7]:

$$F_\alpha = K_m(i_{s2d}\psi_{1d} + i_{s2q}\psi_{1q}) \tag{7}$$

$$F_\beta = K_m(i_{s2d}\psi_{1q} - i_{s2q}\psi_{1d}) \tag{8}$$

Where, $K_m$ is magnetic suspension force coefficient determined by the configuration of bearingless induction motor. $K_m$ can be expressed as following:

$$K_m = \pi L_{m2}/(4\mu_0 lr\mathrm{N}_1\mathrm{N}_2) \tag{9}$$

In equations (7), (8) and (9): $F_\alpha$ and $F_\beta$ are two components of controllable radial magnetic suspension force along stationary $\alpha$ and $\beta$ reference axes; $i_{s2d}$ and $i_{s2q}$ are two current components of two-pole suspension control winding along *d* and *q* rotary reference axes; $\mu_0$ is the magnetic permeability of air; *l* is the length of stator iron core; *r* is the interior radius of stator; $L_{m2}$ is the single-phase excited inductance of three-phase suspension control winding; $N_1$ and $N_2$ are the numbers of turns in series per phase of three-phase four-pole torque windings and three-phase two-pole suspension control windings.

From upper models, it can be seen that: the controllable radial suspension force components $F_\alpha$ and $F_\beta$ are the results of mutual coupling between the airgap magnetic flux-linkage of torque system and the two excited current components of suspension control windings along *d* and *q* reference axes. When rotor flux orientation is adopted for torque system, the required airgap magnetic flux-linkage in equations (7) and (8) can be expressed as equations (10) and (11).

$$\psi_{1d} = L_{m1}(\psi_r + L_{r1l} i_{s1d}) / L_{r1} \tag{10}$$

$$\psi_{1q} = L_{m1} L_{r1l} i_{s1q} / L_{r1} \tag{11}$$

Once the rotor deviate from the stator's centre, the unbalanced distribution of airgap magnetic field in bearingless induction motor will come into being, and the unilateral electromagnetic pull will be produced. The unilateral electromagnetic pull can be expressed as following:

$$f_\alpha = k_s \alpha, \quad f_\beta = k_s \beta \tag{12}$$

In equation (12): $k_s$ is the stiffness coefficient of radial displacement. Then, the radial motion equation of rotor can be expressed as following:

$$m\ddot{\alpha} = F_\alpha - f_\alpha, \quad m\ddot{\beta} = F_\beta - f_\beta \tag{13}$$

Where, *m* is the rotor mass.

According to the dynamic mathematical model of torque system and the radial motion equation of rotor, *etc*., the dynamic model of bearingless induction motor can be derived as following:

$$m\ddot{\alpha} = F_\alpha - f_\alpha \tag{14}$$

$$m\ddot{\beta} = F_\beta - f_\beta \tag{15}$$

$$\dot{\omega}_r = p_1^2 L_{m1} \psi_r i_{s1q} / (J L_r) - p_1 T / J \tag{16}$$

$$\dot{\psi}_r = -\psi_r / T_r + L_{m1} i_{s1d} / T_r \tag{17}$$

## 3. Reversibility Analyses of Three-phase Bearingless Induction Motor System

### 3.1 State control equations of bearingless induction motor system

Firstly, the state variables, input variables and output variables of bearingless induction motor system should be selected as following:

State variables:

$$X = (x_1, x_2, x_3, x_4, x_5, x_6)^T = (\alpha, \beta, \dot{\alpha}, \dot{\beta}, \omega_r, \psi_r)^T \tag{18}$$

Input variables:

$$U = (u_1, u_2, u_3, u_4)^T = (i_{s1d}, i_{s1q}, i_{s2d}, i_{s2q})^T \tag{19}$$

 

Output variables:

$$Y=\left(y_1,y_2,y_3,y_4\right)^T=(\alpha,\beta,\omega_r,\psi_r)^T \tag{20}$$

Put equations (18) ~ (20) into equations (14) ~ (17), then the state equations of system can be derived as following:

$$\dot{x}_1=x_3 \tag{21}$$

$$\dot{x}_2=x_4 \tag{22}$$

$$\dot{x}_3=K_mL_{m1}[(x_6+L_{r1l}u_1)u_3+L_{r1l}u_2u_4]/(mL_{r1})-k_sx_1/m \tag{23}$$

$$\dot{x}_4=K_mL_{m1}[L_{r1l}u_2u_3-(x_6+L_{r1l}u_1)u_4]/(mL_{r1})-k_sx_2/m \tag{24}$$

$$\dot{x}_5=p_1^2L_{m1}x_6u_2/(JL_{r1})-p_1T_L/J \tag{25}$$

$$\dot{x}_6=-x_6/T_r+L_{m1}u_1/T_r \tag{26}$$

From equation2 (20)~(26), it can be seen that: under the condition of rotor flux-linkage orientation of four-pole torque system, the state equations of bearingless induction motor is six order with four order input and four order output. Compared with the state equations of bearingless induction motor that is not oriented, the order number of state equations decreases an order, and the complexity of state equations is weakened respectively [11].

### 3.2 Reversibility analyses of bearingless induction motor system

To analyze the reversibility of bearingless induction motor, according to interactor algorithm, the output variables of $Y=\left(y_1,y_2,y_3,y_4\right)^T$ should be asked the derivative to time gradually, until the input variable $u_j(j=1,2,3,4)$ is obviously included in the derivative function of each $y_i(i=1,2,3,4)$. The detail process can be expressed with following equations:

$$\dot{y}_1=\dot{x}_1=x_3 \tag{27}$$

$$\ddot{y}_1=\dot{x}_3=K_mL_{m1}[(x_6+L_{r1l}u_1)u_3+L_{r1l}u_2u_4]/(mL_{r1})-k_sx_1/m \tag{28}$$

$$\dot{y}_2=\dot{x}_2=x_4 \tag{29}$$

$$\ddot{y}_2=\dot{x}_4=K_mL_{m1}[L_{r1l}u_2u_3-(x_6+L_{r1l}u_1)u_4]/(mL_{r1})-k_sx_2/m \tag{30}$$

$$\dot{y}_3=\dot{x}_5=p_1^2L_{m1}x_6u_2/(JL_r)-p_1T_L/J \tag{31}$$

$$\dot{y}_4=\dot{x}_6=-x_6/T_r+L_{m1}u_1/T_r \tag{32}$$

Assumption:

$$y(u)=(\ddot{y}_1,\ddot{y}_2,\dot{y}_3,\dot{y}_4)^T \tag{33}$$

Then, the Jacobi matrix of bearingless induction motor system can be derived as following:

$$A(x,u)=\partial Y/\partial u^{T}=$$

$$\begin{pmatrix} K_m L_{m1} L_{r1l} u_3/(mL_{r1}) & K_m L_{r1l} u_4/m & K_m L_{m1}(x_6+L_{r1l}u_1)/(mL_{r1}) & K_m L_{m1} L_{r1l} u_2/(mL_{r1}) \\ -K_m L_{m1} L_{r1l} u_4/(mL_{r1}) & K_m L_{r1l} u_3/m & K_m L_{m1} L_{r1l} u_2/(mL_{r1}) & -K_m L_{m1}(x_6+L_{r1l}u_1)/(mL_{r1}) \\ 0 & p_1^2 L_{m1} x_6/(JL_r) & 0 & 0 \\ L_{m1}/T_r & 0 & 0 & 0 \end{pmatrix} \quad (34)$$

In normal operation of bearingless induction motor, $x_6 \neq 0$, $rank[A(x,u)]=4$. Then, the $A(x,u)$ matrix is non- singular; and the relative order of system is: $\alpha=(\alpha_1,\alpha_2,\alpha_3,\alpha_4)=(2,2,1,1)$. More over, the sum of $\alpha_i(i=1,2,3,4)$ equals to 6, *i.e.*, equals to the order of state equations, the bearingless induction motor system is reversible.

## 4. Inverse System Models and Dynamic Doupling Control System

### 4.1 Dynamic mathematical model of inverse system

Selecting the input variable of inverse system as following:

$$Y(u)=\left(\ddot{y}_1,\ddot{y}_2,\dot{y}_3,\dot{y}_4\right)^{T}=\left(\nu_1,\nu_2,\nu_3,\nu_4\right)^{T} \quad (35)$$

According to the implicit function theorem, the inverse system can be expressed as following:

$$u=\phi(x,\nu_1,\nu_2,\nu_3,\nu_4) \quad (36)$$

If the actions of load and outside interference are ignored, the additional integrator realization of inverse system can be expressed as following equations:

$$u_1=T_r\nu_4/L_{m1r}+x_6/L_{m1} \quad (37)$$

$$u_2=L_r(J\nu_3/p_1+T_L)/[p_1 L_{m1r} x_6] \quad (38)$$

$$u_3=L_{r1}[(x_6+L_{r1l}u_1)(m\nu_1+k_s x_1)+L_{r1l}u_2(m\nu_2+k_s x_2)]/\left\{[(x_6+L_{r1l}u_1)^2+(L_{r1l}u_2)^2]K_m L_{m1}\right\} \quad (39)$$

$$u_4=L_{r1}[L_{r1l}u_2(m\nu_1+k_s x_1)-(x_6+L_{r1l}u_1)(m\nu_2+k_s x_2)]/\left\{[(x_6+L_{r1l}u_1)^2+(L_{r1l}u_2)^2]K_m L_{m1}\right\} \quad (40)$$

### 4.2 Dynamic decoupling control system of bearingless induction motor

By series connecting the inverse system in front of the original system, then bearingless induction motor can be compensated to a linear system with four decoupled pseudo linear subsystems. Thereinto the torque system is decoupled into two first order linear integral subsystem, include motor speed and rotor flux-linkage subsystems; and the suspension control system is decoupled into two second order linear integral subsystem, include $\alpha$ and $\beta$ radial displacement subsystems.

Then, aiming at each subsystem, relevant controller is designed, and composite control system is build to enable the system to obtain excellent static and dynamic performance, and obtain anti-jamming capability. Thereinto, motor speed and rotor flux-linkage subsystems adopt PI controller, two radial displacement subsystems adopt PD controller to adjust $\alpha$ and $\beta$ radial displacement components of rotor.

 

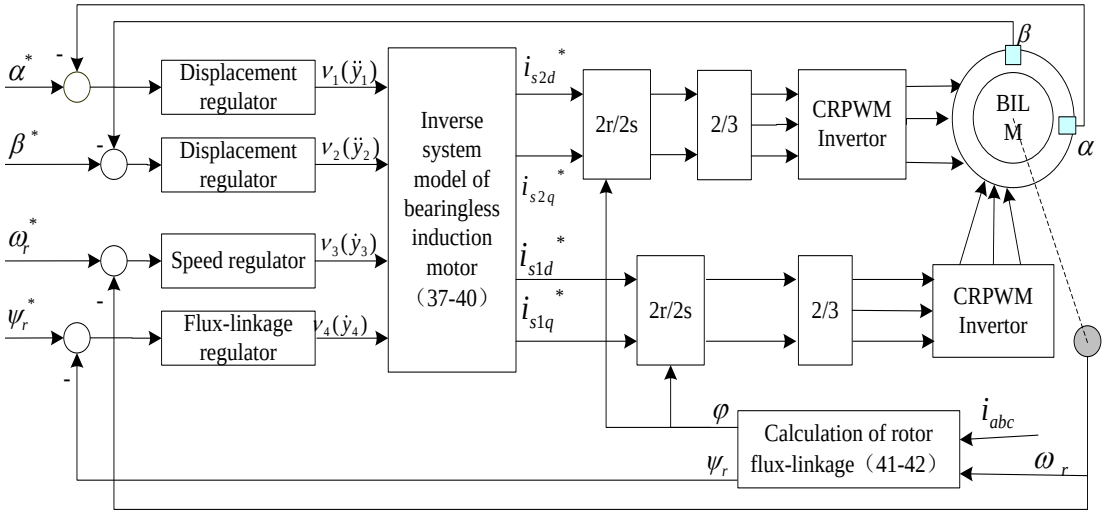


**Figure 2. Dynamic decoupling control system Structure diagram of bearingless induction motor**

Figure 2 shows the structure of dynamic decoupling control system. Thereinto the rotor flux-linkage of torque system can be calculated with following equations:

$$\psi_r = L_{m1} i_{s1d} / (T_r s + 1) \tag{41}$$

$$\varphi = \int (\omega_r + \omega_s) dt = \int [\omega_r + L_{m1} i_{s1q} / (T_r \psi_r)] dt \tag{42}$$

## 5. System Simulation Validation and Analysis

Aiming at the upper analyses, the four-pole bearingless induction motor with two-pole suspension control windings is taken as the research object. According to the control system structure in Figure 2, simulation research has been made by Matlab/Simulink.

Parameters of bearingless induction motor:

1) Stator inner diameter $r$=62mm; the effective core length of bearingless induction motor $l$ =0.82mm; motor airgap length $\delta_0$=0.6mm; Auxiliary bearing air gap $\delta_1$=0.2mm.

2) Torque system: $P$=2.2kW, stator winding resistance $R_s$=1.6Ω, rotor winding resistance $R_r$=1.423Ω, leakage inductance of stator windings $L_{s1l}$=0.0043H, leakage inductance of rotor windings $L_{r1l}$=0.0043H, excited inductance of torque windings $L_{m1}$=0.0859H, and the rotation inertia of motor $J$=0.024 kg.m2.

3) Suspension system: stator winding resistance $R_{s2}$= 2.7Ω, leakage inductance of stator windings $L_{s1l}$=0.00398H, leakage inductance of rotor windings $L_{r1l}$=0.00398H, excited inductance of suspension windings mutual $L_{m2}$=0.230H.

Setting simulation conditions as following:

1) The initial radial displacements of rotor $\alpha_0$=-0.12mm, $\beta_0$=-0.16mm; given value of rotational speed $n^*$=1500r/min, given value of rotor flux-linkage $\psi^*_r$ = 0.95Wb, given value of radial displacements $\alpha^*=\beta^*=0$. The motor starts with no-load.

2) To validate the dynamic decupling performance of control system, several given signals, including $\alpha^*$, $\beta^*$, $\psi^*_r$ and $n^*$, will be changed suddenly in the simulation process.

Figure 3 shows the simulation waveforms of dynamic decoupling control system of three-phase bearingless induction motor. Thereinto, Figure 3(a) to Figure 3(d) present the dynamic response curves of motor speed, rotor flux-linkage, $\alpha$ radial displacement and $\beta$ radial displacement respectively. And Figure 3(e) shows the given curve of load torque. From the simulation results in Figure 3, it can be seen that:

1) In the non-load starting process of bearingless induction motor, the motor speed reach to its given reference value within 0.1s, and has no overshoot; the rotor flux-linkage has little overshoot, but it can reach to steady state within 0.2s; After a slight fluctuation, two radial displacement components, *i.e.*, $\alpha$ and $\beta$, can accurately track the given values within 0.1s, the fast and stable suspension of bearingless induction motor has been achieved.

2) To verify the decoupling performance between torque system and suspension system, and that between motor speed and rotor flux linkage, the given value of rotor flux-linkage is decreased to 0.38Wb at 0.4s, and the given value of motor speed be increased to 3750r/min, i.e. the working frequency be increased to 125Hz at 0.8s. From Figure 3(a) to Figure 3(d): in the sudden change processes of motor speed and rotor flux-linkage, $\alpha$ and $\beta$ radial displacements component have no change basically. Simulation results have shown that better dynamic decoupling performance has been achieved between torque system and suspension system.

3) From Figure 3(a) to Figure 3(b): in the sudden change process of rotor flux-linkage, the motor speed almost has no change; and in the sudden change process of motor speed, there has little change in rotor flux-linkage. Simulation results have shown that better dynamic decoupling control has been achieved between motor speed subsystem and rotor flux-linkage subsystem.

4) To verify the decoupling performance between two radial displacement control subsystems, the radial displacement given value α* suddenly changes from 0.0 to 0.04mm or 40μm at 1.2s, and at 1.35s, the given value α* returns to the zero. The radial displacement given value β* suddenly changes from 0 to -0.04mm or -40μm at 1.6s, and the given value β* returns to the zero at 1.75s. According to Figure 3(c) to Figure 3(d): in the change processes of α and β, there almost has no coupling between each other. The simulation results have shown the higher dynamic decoupling control performance between α and β radial displacement subsystems.

 

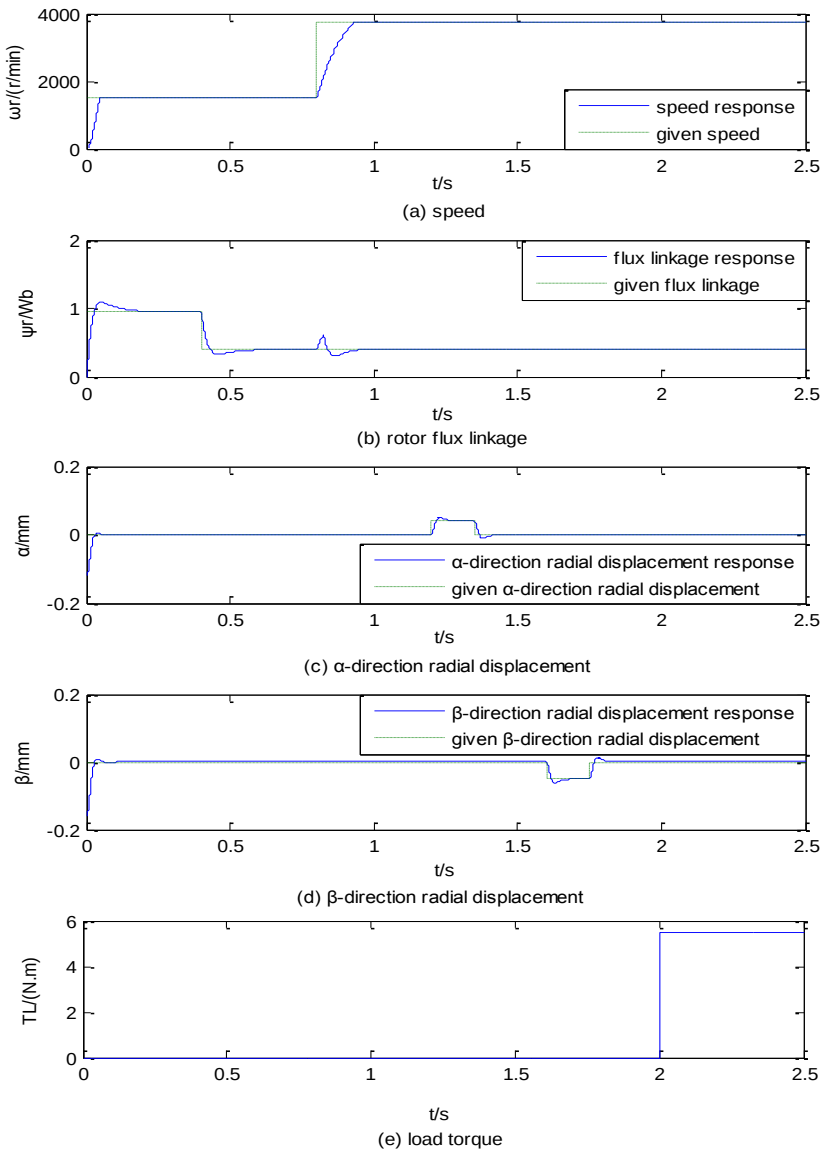


**Figure 3. Response curves of decoupling control system of bearingless induction motor**

5) According to Figure 3(a) to Figure 3(e), when $5.5\,N\cdot m$ torque load is added on the control system of bearingless induction motor at 2.0s, the motor speed, rotor flux-linkage, $\alpha$ and $\beta$ radial displacements component have no change basically. The simulation results not only have verified the dynamic decoupling control performance between torque system and suspension control system in farther step, but also have shown the stronger anti-interference ability of the control system.

## 6. Conclusion

Three-phase bearingless induction motor is a multi-variable, nonlinear and strong coupling object. To achieve its high performance control, the dynamic mathematical model of three-phase bearingless induction motor has been analyzed firstly; then the reversibility of the

overall bearingless induction motor system were discussed in detail, and based on the rotor flux orientation of torque system, the dynamic mathematical models of inverse system of three-phase bearingless induction motor were derived. And adopting inverse system decoupling control theory and method, the three-phase bearingless induction motor were compensated to four decoupled pseudo linear subsystems, include motor speed, rotor flux linkage, $\alpha$ and $\beta$ radial displacement components, *etc*. After then, using the design method of linear systems theory, the controller of each pseudo linear subsystem has been designed. The overall inverse dynamic decoupling control system structure has been presented, and overall system simulation research and verification have been made.

According to the simulation results, stable dynamic decoupling between torque control system and suspension control system can be achieved. More over, within torque system, the dynamic decoupling between motor speed and rotor flux-linkage control subsystem has been achieved; and within suspension control system, stable dynamic decoupling between $\alpha$ and $\beta$ radial displacement component control subsystems has been achieved also. The decoupled control system of three-phase bearingless induction motor has the characteristics of fast dynamic response and stronger anti-interference ability. The presented inverse dynamic decoupling control strategy is validate and feasible. Thus the theory foundation has been laid for the research and design of high performance decoupling controller of three-phase bearingless induction motor.

## Acknowledgements

The supports of International Cooperation Project on Science and Technology of Henan Province (114300510029), National Natural Science Foundation of China (51277053), and Nature Science Fund of Henan Province Education Bureau (2010B510011), are acknowledged.

## References

[1] A. Chiba and J. A. Santisteban, "A PWM Harmonics Elimination Method in Simultaneous Estimation of Magnetic Field and Displacements in Bearingless Induction Motors", IEEE, Trans on Industry Applications, vol. 48, no.1, **(2012),** pp. 124-131.
[2] J. Asama, Y. Hamasaki and T. Oiwa, "Proposal and Analysis of a Novel Single-Drive Bearingless Motor", IEEE, Trans on Industrial Electronics, vol. 60, no. 1, **(2013)** , pp. 129-138.
[3] V. F. Victor, F. O. Quintaes and J. S. B. Lopes, "Analysis and Study of a Bearingless AC Motor Type Divided Winding Based on a Conventional Squirrel Cage Induction Motor", IEEE, Trans on Magnetics, vol. 48, no. 11, **(2012)**, pp. 3571-3574.
[4] W. S. Bu, S. H. Huang and S. M. Wan, "General Analytical Models of Inductance Matrices of Four-Pole Bearingless Motors with Two-Pole Controlling Windings", IEEE, Trans on Magnetics, vol. 45, no. 9, **(2009)**, pp. 3316-3321.
[5] E. F. Rodriguez and J. A. Santisteban, "An Improved Control System for a Split Winding Bearingless Induction Motor", IEEE, Trans on Industrial Electronics, vol. 58, no. 8, **(2011)**, pp. 3401-3408.
[6] A. Chiba and J. Asama, "Influence of Rotor Skew in Induction Type Bearingless Motor", IEEE, Trans on Magnetics, vol. 48, no. 11, **(2012)**, pp. 4646-4649.
[7] W. S. Bu, S. J. Wang and S. H. Huang, "Decoupling control system of three-phase bearingless induction motor", Electric Machines and Control, vol. 15, no. 12, **(2011)**, pp. 32-37, 4.
[8] V. F. Victor, F. O. Quintaes and J. S. B. Lopes, "Analysis and Study of a Bearingless AC Motor Type Divided Winding, Based on a Conventional Squirrel Cage Induction Motor", IEEE, Trans on Magnetics, vol. 48, no. 11, **(2012)**, pp. 3571-3574.
[9] X. D. Sun and H. Q. Zhu, "Decoupling control of bearingless induction motors based on neural network inverse system method", Transactions of China Electrotechnical Society, vol. 25, no.1, **(2010)** , pp. 43-49.
[10] Z. Q. Wang and X. X. Liu, "An improved rotor flux oriented control system of bearingless induction motors", Proceedings of Chinese Control and Decision Conference, (**2010)**, pp. 2733-2737.

 